

DEVELOPMENT OF A PROCEDURE TO DETERMINE INTERNAL STRESSES IN CONCRETE BRIDGE MEMBERS

Steven F. Hammerschmidt, Kansas State University, Manhattan, Kan.

Robert J. Peterman, Ph.D., P.E., Kansas State University, Manhattan, Kan.

Weixin Zhao, Ph.D., Kansas State University, Manhattan, Kan.

B. Terry Beck, Ph.D., Kansas State University, Manhattan, Kan.

John Wu, Ph.D., Kansas State University, Manhattan, Kan.

ABSTRACT

With aging and deterioration of bridges, evaluation of existing conditions of their structural elements becomes vital to engineers and public officials when deciding how to repair or replace the structures. The ability to obtain necessary information on these conditions is often expensive and time consuming, especially for concrete bridges where the reinforcement is not accessible for inspection. Employing the surface-strain relief method could allow for accurate evaluation of aged or damaged prestressed members.

The surface-strain relief method was developed to measure initial or pre-existing strains in a member. It involves relieving the strain in the member and measuring change in strain. Two methods were tested—one used a linear electrical-resistance strain gage and a three-inch-diameter diamond concrete core bit to core around the gage, and the second method used a laser-speckle imaging device and a diamond cutting wheel to cut notches perpendicular to the axis of maximum strain. Both methods measured the change in strain and related it to within 10 percent of the actual f_{se} . The method of cutting notches and the laser-speckle imaging device provided a simpler method to be implemented in the field, while the coring method achieved a higher level of accuracy and precision.

Keywords: Assessment and Monitoring, Repair and Rehabilitation, Research

INTRODUCTION

In North America, many prestressed concrete bridges have been built over the past five decades. Many of these bridges are coming up on the end of their design life or have been subjected to larger loads and heavier traffic demands, making them deficient and in need of repair. To preserve the structural integrity of the bridges and safety of the public, inspections need to be conducted. With prestressed members, visible inspections are not sufficient to determine the condition of the structure due to environmental and time-dependent losses of the prestressing force. Therefore, engineers need a reliable method to determine the remaining prestress force in a member during routine inspections, rehabilitation, or when retrofitting the structure.

With aging infrastructure, it becomes increasingly important to calculate or measure the remaining prestress force in existing structures. Often times when trying to calculate the remaining prestress force, limited information exists on actual design and/or construction and environmental conditions. Thus, assumptions have to be made affecting the accuracy of the analysis. Insignificant initial flaws in the members can go unnoticed but due to time-dependent losses, over time these can become critical to the strength of the member. Prestress force is a time-dependent phenomena influenced by factors such as elastic shortening due to transfer, shrinkage, creep, and relaxation that occurs after transfer. These losses are calculated based on geometric and mix properties of the member, along with environmental conditions. Based on research, equations have been developed to enable the calculation of losses over time. These equations are not exact and are only estimates, and have been developed to provide estimates for many types of prestressed members.

With these factors in mind, a method of surface-strain relief was developed to accurately measure the remaining prestress force through residual stresses while being mostly non-destructive. The method allows bridge members to be checked over time to ensure the members are still meeting the design assumptions. Calculation of the losses is only an estimate, so the surface-strain relief method could lengthen the life of a structure by providing a level of confidence that the structure can still perform as designed. The surface-strain relief method provides a cost-effective means to evaluate the condition of the structure, and places a higher level of certainty on decisions by owners and engineers in regard to the condition of the structure. Bridge owners can then make informed decisions about how to allocate maintenance funds and reduce the inherent risk associated with deteriorating infrastructure with this information.

DESCRIPTION OF TEST BEAMS

A total of six beams were tested with the surface-strain relief method at multiple locations along each beam. Four beams were cast at Kansas State University (K-State), and two nine-year-old T-beams were tested using the developed method. The beams cast at K-State and shown in Fig. 1 had a cross-section of six inches wide by 12 inches tall and 120 inches in length. Reinforcement in each beam consisted of two, ½-inch 270 ksi low-relaxation strands

stressed to 160 ksi. The low prestressing force allowed the method to evaluate a stress that would be close to f_{se} after all long term losses for a typical member. Two, 1/2-inch 50 ksi steel reinforcing bars, to control the tensile stress, were placed two inches from the top of the beam. Four stirrups were used to hold the top bars in place.

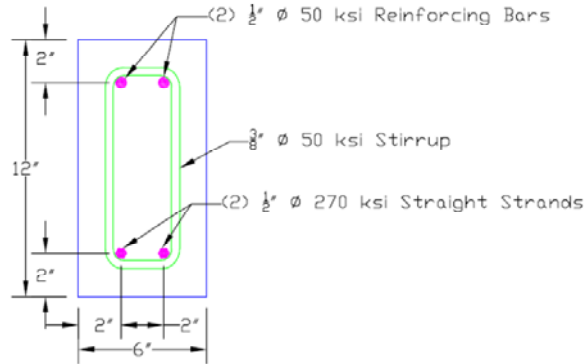


Fig. 1 Cross-Section of Beams Cast at K-State

The four rectangle beams were cast in two separate pours using the same materials and design mix. Each mix had design 28-day strength of 6000 psi and required release strength of 4200 psi. Table 1 shows properties of the rectangle beams tested. Compressive strengths were taken at 28 days, and the modulus of elasticity was determined from test cylinders according to ASTM C 469¹. Average prestress force was calculated by measuring the losses of each beam and verifying those by determining the load required to open a crack at the base of beam^{2, 3}. The prestressing steel had a tensile strength of 270 ksi and a modulus of elasticity of 28,500 ksi. The top bars and stirrups had a tensile strength of 50 ksi with a modulus of elasticity of 29,000 ksi.

Table 1 Beam Properties

| Beam | Average Compressive Strength (psi) | Modulus of Elasticity (ksi) | Average Prestress Stress (ksi) |
|------|------------------------------------|-----------------------------|--------------------------------|
| 1a | 7490 | 3750 | 134.8 |
| 1b | 7490 | 3300 | 135.0 |
| 2a | 7390 | 3950 | 114.5 |
| 2b | 7390 | 3550 | 98.0 |

The prestressed concrete T-beams were cast at a local precast plant in March of 2002. The T-beams had a top flange 18 inches wide and four inches deep, with a tapered web four inches wide at the bottom, and a total depth of 14 inches (see Fig. 2). The T-beams had two straight 3/8-inch 270 ksi low relaxation strands, one two inches up and another four inches up from the bottom and jacked to a stress of 202.5 ksi. Additional mild reinforcement of D4 welded wire reinforcement was placed in the beam at 1.25, 3, 4, and 7 inches from the top. Shear reinforcement was provided in the form of D4 welded wire reinforcement placed four

inches on centers in the flange and D6 welded wire reinforcement placed four inches on center in the web.

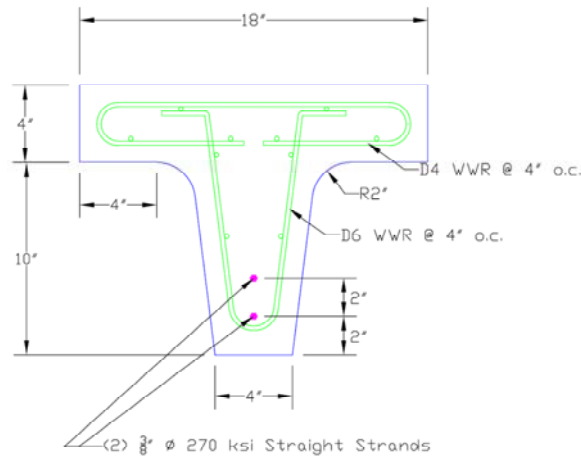


Fig. 2 T-Beam Cross Section

The T-beams were produced in 2002 at a prestressed plant in Kansas. The plant provided concrete strengths of the concrete through standard cylinder testing⁴. The average 28-day strength was found to be 7,043 psi. The 3/8-inch strand used in the beams had a tensile strength of 270 ksi and an elastic modulus of 28,300 ksi. The additional mild steel reinforcement had a tensile strength of 80 ksi and an elastic modulus of 29,000 ksi. Average prestress stress was calculated following the same procedure to verify losses on the beams cast at K-State. During loading of the beams, the mid-span deflection was measured and used to compute the modulus of elasticity of the beam from the load and mid-span deflection⁵. Properties of the T-beam are shown in Table 2.

Table 2 T-Beam Properties

| T-Beam | Modulus of Elasticity (ksi) | Average Prestress Stress (ksi) |
|--------|-----------------------------|--------------------------------|
| 1 | 3550 | 129.3 |
| 2 | 3000 | 146.0 |

SURFACE-STRAIN RELIEF METHOD

The surface-strain relief method measures residual stress on the surface of a member and relates it to the prestress force in the member. The surface-strain relief method has four main steps:

- 1) Measuring initial strain
- 2) Coring or cutting notches
- 3) Measuring relaxation of the concrete
- 4) Relating relaxation of the concrete to the average prestress force

Two methods were explored to measure the surface strain—traditional linear electrical-resistance strain gages and a laser-speckle imaging (LSI) device that was developed at Kansas State University⁶. Initially, residual stresses on the surface were relieved by coring around the strain gage, but upon further research, a method of notching was used and showed promising results. The core and notches were cut to varying depths to determine optimal depth and compared with finite-element models. The strain was measured after each incremental core or notch depth. Change in strain was assumed to be the relief of the residual stress and was used to calculate the average prestress force in the member.

MEASUREMENT OF STRAIN

Two methods were used to measure the surface strain—the traditional linear-resistance strain gages and the LSI device. The linear resistance-strain gages were used with the concrete diamond coring bit and with the notches. The LSI device was not used with the core because it measures the strain over a larger area, requiring a larger core bit. A larger core would provide many disadvantages to the method, and limit possibilities and applications. With the larger gage length and development of the notches, the LSI device provided an opportunity to simplify the method.

With either method, the linear electrical-resistance strain gage or the LSI device, the strain is only measured in one direction. In order to get the least error and the largest change in strain, the strain gage or the LSI device must be positioned parallel to the axis of maximum strain. For the interest of this project, the remaining prestress force was being investigated, so the gages were positioned along the centroid of the prestress strand.

The first method to measure strain was the traditional method using linear electrical-resistance strain gages. Due to the heterogeneous nature of concrete, a two-inch gage length was used, which was approximately five times larger than the diameter of the largest aggregate in the mix⁷. The beam surface was initially prepared by removing any laitance from the surface then filling all voids with epoxy. Once the epoxy was cured, the gage was mounted to the prepared surface using the same epoxy. Installation of the strain gage followed the standard procedure but consideration was needed when connecting the leadwires. A core was going to be cut around the strain gage, and the leadwires needed to be protected to ensure they were not damaged during coring. To protect the wires, a four-pin

terminal block was attached to the strain gage and secured to the center of the core, using silicone to hold it in place as shown in Fig. 3 prior to placing the silicon, the gages were protected by using a polyurethane coating followed by a coat of microcrystalline wax.



Fig. 3 Strain Gage with Terminal Block Mounted Using Silicon

The second method used the LSI device, which uses the surface of the beam to measure the change in displacement. The device images the speckle pattern produced by a laser reflecting off the surface, producing a unique pattern from the member's surface and serving as a fingerprint of the location. Two locations are imaged simultaneously initially to serve as the reference point. Subsequent measurements are correlated to the reference images to find the amount of displacement. A strain gage was compared to the LSI device as shown in Fig. 4, showing the high level of accuracy of the device.

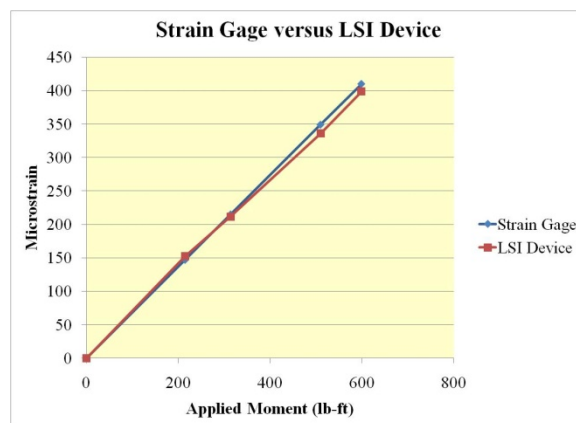


Fig. 4 Comparison of Strain Gage to LSI Device

The device shown in Fig. 5 is attached to brackets which allow the device to be easily removed from the beam, and then repositioned on it. The closer the device is positioned to its original location, the higher its level of accuracy and the less error introduced into the measurement. To aid in the placement of the device and maintain the distance away from the surface, two brackets were fabricated to be attached to any surface, while remaining out of the way for the notch-cutting process. The brackets were attached using a five-minute epoxy.

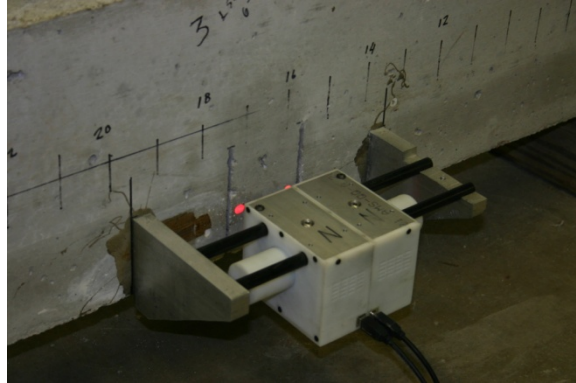


Fig. 5 LSI Device Attached to Beam

The device uses the surface of the concrete to determine the displacement. Extra care was taken to preserve the concrete surface and not damage it, as changes to the concrete surface would destroy correlation with the LSI device. The surface was cleaned using a wire brush and compressed air before imaging the reference reading. Tape and plastic were used to cover the surface, having the tape only touch the surface of the beam near the notch and not where the surface would be imaged, to protect the surface while cutting notches in the concrete.

CORING PROCESS

The coring process relieves the stress inside the core, allowing for a relief of strain, which is measured by the strain gage. Relief of the strain is dependent on the depth of the core, so multiple core increments were used to determine the optimal depth. A three-inch diameter core bit was used to core around the two-inch gage, to allow the core to be cut close to the edge of the strain gage but not to damage the gage. No water was used during the coring process, which would affect the measured strain due to swelling of the concrete caused by the water^{8,9}. To correct for the temperature increase from the coring process, a non-contact thermometer was used to measure the temperature in and around the core.

The first step of the coring process was to balance all gages to zero microstrain. Gages were mounted at various locations on each beam, including gages on each side of the beam. Figure 6 shows the location of the gages on one side of the beam, with the gages on the other side positioned between the gages on the other side of the beam, so no two gages align. All gages were excited with two volts through a strain indicator used in conjunction with a switch-and-balance unit to monitor the multiple strain gages. Once the gages had been zeroed with the switch-and-balance unit, the terminal block was disconnected from the gage and then reattached to record any difference in strain that was caused from the connection. An error of ± 1 microstrain was recorded as the maximum error observed from the terminal block connection. Next, the lead wires were disconnected and checked to ensure they were securely attached to the center of the core. Layout marks from the positioning of the strain gage were extended in order to position a guide for the diamond core bit. A wooden guide was built using $\frac{3}{4}$ -inch particle board, with a stop on the bottom to help in locating the center of the core. Using the provided layout marks, the guide was next mounted on the surface of

the beam and centered on the strain gage. A hole was cut slightly larger than the diameter of the core bit to allow it to spin freely within the guide. The guide prevented the bit from moving on the surface of the beam as the coring process started and prevented the possibility of damaging the gage. To prevent excess friction and keep the amount of concrete dust to a minimum, a vacuum was used near the core hole to remove the concrete dust. When a depth of 0.5 inch was reached, a caliper was used to measure the depth of the core in multiple locations. This ensured the core was being cored at a uniform depth and perpendicular to the surface. The coring was then continued to 0.75 inch where the depth was checked again and a strain reading was taken. Ten minutes were allowed between coring increments to minimize temperature effects on the strain readings. After the final depth of one inch was reached, a final reading was taken 10 minutes after the coring was complete. Fig. 7 shows the result of the coring process.

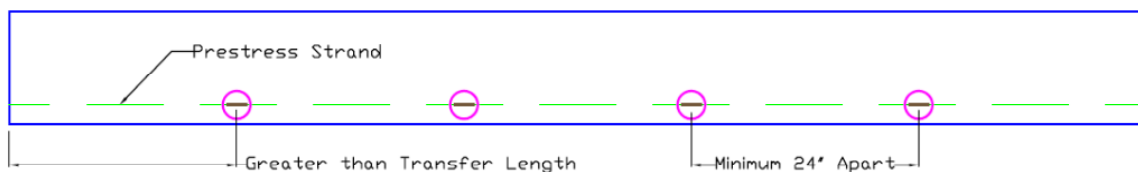


Fig. 6 Location of Cores

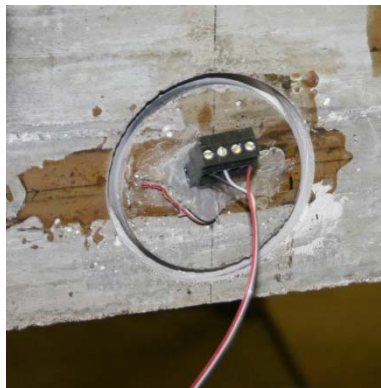


Fig. 7 Completed Core

To investigate effects of temperature and the error induced in the strain measurements, a non-contact thermometer was used to measure the temperature of the surrounding environment and the beam throughout the coring process. Temperature measurements of the beam, core, and the ambient temperature were taken initially, after each coring increment, and 10 minutes after each coring increment. A maximum temperature increase of 40° Fahrenheit was seen with an average temperature increase of 30° Fahrenheit. After 10 minutes, the core temperature was within 10 degrees of ambient temperature. To calculate the error caused by the thermal increase, thermal output coefficients from the strain gage's technical data were used in a regression-fitted polynomial equation¹⁰. Using the obtained polynomial curve for the thermal output, the change in strain reading was calculated due to the increase in the temperature, shown in table 3. Some of the cores showed this increase, while other gages

seemed to take a few minutes to come to equilibrium due to the release of strain. Many of the cores showed a decrease in strain after the one-inch increment where only a small increase in relieved stress took place. With this data, the increase in temperature did not significantly affect the measured strain. The rest of the cores were not monitored for temperature increase but were allowed to reach equilibrium with the beam temperature for 10 minutes before a final strain reading was taken.

Table 3 Strain Increase Due to Temperature Fluctuations

| | Average Δ Temperature ($^{\circ}$ F) | Increase in Strain ($\mu\epsilon$) |
|------------------|---|---|
| 3/4" depth | 30 | 22.5 |
| After 10 minutes | 9 | 9.5 |
| 1" depth | 20 | 17.8 |
| After 10 minutes | 3 | 3.4 |

NOTCHING PROCESS

The notching process provided a simpler and quicker method of relieving the stress at the surface. It involved cutting a notch on both sides of the strain gage at a distance of 1.75 inches from the center of the gage. The notching process was similar to the coring process for measuring the strain at different increments. Multiple depths were tried to determine the optimum depth. The notches were cut using a five-inch diamond wheel designed for dry cutting applications and to be used with a handheld grinder. A variable depth and dust extraction guard were used on the grinder to control the depth of the cut and to minimize the dust created. The guide also maintained the blade perpendicular to the surface of the concrete.

Initial balancing of the strain gage was the same as the core procedure, with the gage balanced to zero. Unlike the core procedure, a terminal block connection on the lead wires was not needed. The wires could remain connected to the strain gage at all times, but needed to be secured out of the way to prevent the wires from being cut. Spacing between the two notches was set at 3.5 inches. This spacing allowed for ample room between the notch and the edge of the strain gage to prevent the possibility of the edge of the cut chipping out and damaging the gage. This spacing was also used with the LSI device. With the LSI device, initial readings had to be taken once the mounting brackets and surface were prepared. A set of 10 reference readings were taken and an average of all 10 was used in calculating the prestressing force. To ensure high-quality reference readings were taken, another set of measurements was taken after the reference readings. To take the second set of readings, the device was removed from the mounting brackets and then repositioned. Once repositioned, another 10 measurements were taken.

From the center of the gage, a line was drawn 1.75 inches from each side of the center and three inches past the uppermost prestressing strand. The line served as a reference for where to cut. Cutting three inches past the uppermost prestressing stand allowed for a full depth of

cut one inch past the strand, and represented the curvature of the blade and the intersection on the surface at a cut depth of one inch. Depths of 0.75, one, and 1.25 inches were cut, allowing five minutes between each notch depth to allow the gage to stabilize (Fig. 8 shows the notches after using the LSI device).

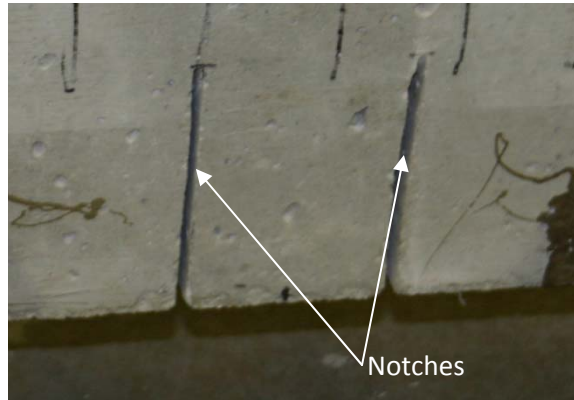


Fig. 8 Notches Complete using the LSI Device

To investigate effects of temperature on the notching procedure, the noncontact thermometer was used. With the noncontact thermometer, initial temperatures of the beam, location of the notches, and ambient temperatures were taken. After the notching was complete, a maximum temperature increase of five degrees Fahrenheit was found. Within a few minutes, the temperature around the notches was found to be in equilibrium with the surrounding beam. This temperature was much lower than the coring temperature increase, and the temperature increase of five degrees provided minimal strain drift.

CALCULATION OF THE AVERAGE PRESTRESS FORCE

To find the average prestress force in the beam, the measured relaxation of strain had to be converted to a change in stress, which was then related to the stress in the concrete. The measured strain is a tensile stress, but the stress on the beam is a compressive stress so a sign change is needed. Using the calculated modulus of elasticity, the strain relieved was converted by Hooke's Law, assuming the concrete is linear elastic.

$$\sigma = E \cdot \varepsilon \quad (1)$$

where E is the calculated modulus of elasticity based on the calculated modulus, and ε is the measured relieved strain on the surface of the beam. The prestress force was then solved for the calculated stress according to the equation:

$$\sigma = -\frac{P}{A} - \frac{Pec}{I} + \frac{Mc}{I} \quad (2)$$

where P , the average prestress force, was solved for A as the cross-sectional area, e as the prestress force eccentricity, c as the distance from the neutral axis to the center of the core, I

as the moment of inertia, and M as the moment due to the mass of the beam and any additional dead load on it.

FINITE-ELEMENT MODELS

To visualize the stress distribution and test many different combinations of core depths and notch configurations, finite-element models were created using Abaqus CAE software. The models represented the prestress members used for the laboratory experiments with similar dimensions and material properties. Each model initially was created without a core and compared to the theoretical stress calculated in the prestress member, determining that the model was built accurately, and then adding either a core or two notches at the mid-span of the beam.

Initially a base model was created with the same cross-sectional properties as the laboratory specimens. The beams were restrained in the model similar to a simply supported beam with one end pinned and the other end supported on a roller. The prestressing strands were represented by stringers with equal area to a strand, and each had an initial stress of 150 ksi. An elastic modulus of 3,100 ksi for the concrete, with a Poisson's ratio of 0.2 and 28,500 ksi for the prestress steel elastic modulus and a Poisson's ratio of 0.3, were the only material property entered into Abaqus. Tensile and compressive strengths were not included into the models due to the fact that no stress exceeded yield or fracture points, and it was assumed that all materials behaved linear elastically. Other transverse reinforcement was omitted from the models, and it was assumed the reinforcement had little effect on the cores, unless a core was over the reinforcement.

The mesh for each model consisted of beam elements for the prestressed strand and structural hex elements for the rest of the model. Partitions were created around the core or notch to create a finer mesh in this area of interest. This refinement was used to reduce the computational time of each model. Each model had approximately 15,000 elements, with the finer mesh having an approximate element size of 0.25 inches and the rest of the model having an approximate mesh size of one inch.

Multiple models were created starting with the rectangle beams as a base model, with varying depths of cores and notches. The first three models had cores in the side of the beam with three varying depths, 0.75, one, and 1.25 inches. The cores were represented by removing the material between the inner and outer diameter of the core bit, leaving a cylindrical ring cut out. For the notches, a spacing of 3.5 inches was set as the distance between them. The first model created had a notch depth of 1.25 inches, with spacing between notches of 3.5 inches. The notch was modeled as a cut three-inches long at the bottom of the notch, creating total length on the surface of approximately five inches. Other depths of notches included one inch and 1.125 inches, along with varying the spacing between the notches and the length of the notch.

RESULTS

All models started from the same base model and contained the same parameters so they could be compared directly to one another. To compare the models, stresses were measured at each node location along the center of the core or notch. This area along the center of the core or notch would also be where the strain measurement would be taken with a strain gage or LSI device. To determine the residual stress that would be measured by a strain gage or the LSI device, the stress values were plotted and Simpson’s rule was used to calculate the area under the curve where the strain gage would be positioned. The stresses near the edges were near zero as expected, but a tensile stress increase followed with a decrease in stress to the midpoint. To get a full relaxation, the tensile stress needed to be balanced out by the compressive stress towards the midpoint of the core, as shown in the plot of the varying depth of cores in Fig. 9.

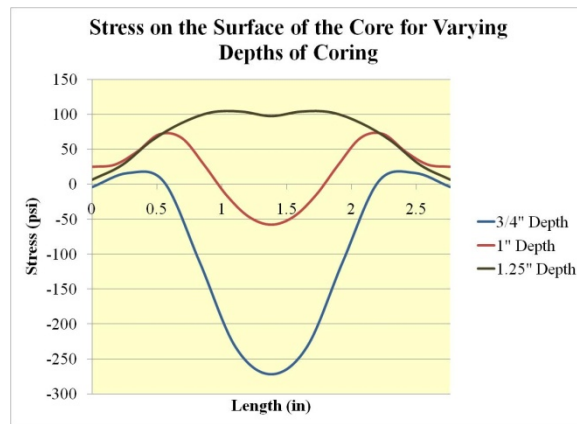


Fig. 9 Plot of Stress on Surface of Core

Table 4 shows the depth of the core and the calculated stress using Simpson’s Rule, along with the percent of relieved stress. The percent of relieved stress was calculated from the stress of -1490 psi, which was found on the non-cored beam two inches up at mid-span of the beam. Both Table 4 and Fig. 8 show that 0.75-inch core depth does not provide a full relaxation of the stress and that the 1.25-inch core depth provides a full relaxation, but some induced bending stresses resulted causing a measured tensile stress, which over predicts the amount of applied prestress force. The one-inch core depth balanced out the compressive stresses and tensile stresses, providing a near 100% relief of stress, just slightly overestimating the prestressing force.

Table 4 Calculated Stresses and Percent Relieved of Cores

| Core Depth (in) | Simpson's Rule Calculated Stress (psi) | % Relieved Stress |
|-----------------|--|-------------------|
| 0.75 | -266 | 82% |
| 1 | 15 | 101% |
| 1.25 | 174 | 112% |

Stresses relieved by the notches were more dependent on depth than on the cores (see Table 5). Spacing between the two notches was kept at a constant length, along with the total length of each notch. A similar stress distribution was seen as with the cores, with both tensile and compressive stresses along the surface. A depth of 1.125 inches was found to represent a full stress relief as seen in Table 5. A change in depth of ± 0.125 inch results in a large change in relieved stresses, either under or overestimating the residual stresses.

Table 5 Calculated Stresses at a Spacing of 3.5", Length of 3", and Varying Depth

| Notch Depth (in) | Simpson's Rule Calculated Stress (psi) | % Relieved Stress |
|------------------|---|----------------------|
| 1 | -352.85 | 76% |
| 1.125 | 3.97 | 100% |
| 1.25 | 317.93 | 121% |

There were more variables to the notching procedure to relieve the stress than just the depth of the notch. To look at the other variables three models were created examine the spacing of the notches and three models view the length of the notches. Three models varied the total length of the notch that was cut to the full depth of one inch. The lengths looked at were two, three, and four inches, while keeping the spacing at 3.5 inches and a depth of one inch. As Table 6 shows, lengths of two and three inches are very similar, with a length of four inches relieving the least amount of stress. Next the spacing between the notches was modified to see its effects on the relieved stresses. Three spaces of 2.5, 3, and 3.5 inches were compared using a constant depth of one inch and a length of three inches. As the spacing got closer together, the amount of relieved stress increased. At a spacing of 2.5 inches, influences of each notch seemed to influence the relieved stress, creating a positive tensile residual stress between the notches. Table 7 shows the calculated stresses and the percent of relieved stress. A spacing of three inches seems acceptable, with a 5% error, when a one-inch-depth notch is cut.

Table 6 Calculated Stresses at a Notch Depth 1", Spacing of 3.5", and Varying Lengths

| Notch Length (in) | Simpson's Rule Calculated Stress (psi) | % Relieved Stress |
|-------------------|---|----------------------|
| 2 | -351.47 | 76% |
| 3 | -352.85 | 76% |
| 4 | -689.35 | 54% |

Table 7 Calculated Stresses at a Depth of 1", Length of 3", and Various Spacing

| Notch Spacing (in) | Simpson's Rule Calculated Stress (psi) | % Relieved Stress |
|--------------------|---|----------------------|
| 2.5 | 283.18 | 119% |
| 3 | 81.45 | 105% |
| 3.5 | -352.85 | 76% |

The two combinations that balance out the tensile and compressive stresses between the notches are a depth of one inch and a spacing of three inches, or a depth of 1.125 inches and a spacing of 3.5 inches, each having a ratio of approximately 0.33. This ratio could be used if different beams were to be tested, and the depth or spacing needed to be changed. For the surface-strain relief method, a spacing of 3.5 inches was chosen to allow ample space around the strain gage and to allow for use of the LSI device, which had a larger gage length.

All of the previous models used beams with a rectangle cross section. To see the validity of the depths and spacing, the T-beams were modeled next with the three-inch core at a depth of one inch, and the notches at a depth of 1.125 inches and a spacing of 3.5 inches. From results of the finite-element models of the T-beams, it can be seen that the optimal depths and notch configurations determined from the other finite-element models will also apply to the T-beam and provide an acceptable relief stresses. Table 8 shows the stresses that remain on the surface of the core or notch and what percentage of stress is relieved compared to the applied prestressing force.

Table 8 T-Beam Results

| Method | Simpson's Rule Calculated Stress (psi) | % Relieved Stress |
|--------|---|----------------------|
| Core | 20.53 | 103% |
| Notch | 64.85 | 109% |

SURFACE-STRAIN RELIEF METHOD RESULTS

Each beam had multiple cores or notches made at different locations along both sides of the beam. Each location was offset from the location on the opposite side of the beam so two test locations would not line up, which would reduce the cross-sectional area at that location. A reduced cross-sectional area would result in an increase in the measured strain and affect the accuracy of the measurement. The initial set of beams tested was 1a and T-beam 1, which used the core method. Other beams tested used a combination of methods to compare the results of each. Beams 1a and 2a were tested within the first three months after the beam was cast, and beams 1b and 2b were tested between eight and 10 months after. T-beams 1 and 2 were approximately nine years old at the time of testing.

The first beam cored was beam 1a, and four gages were successfully cored. Due to the tight tolerances between the strain gage and the edge of the core, one gage was damaged while coring and another gage experienced substantial drift during the process. Table 9 shows the measured strains on beam 1a at 0.75 inch and one inch in depth. The cores were taken at various locations along each side of the beam varying the theoretical strain due to the self-weight of the beam. The surface-strain relief method gave consistent results on beam 1 at varying depths, as with the other beams.

Table 9 Measured Strains on Beam 1a

| Core | Theoretical ($\mu\epsilon$) | 3/4" Depth ($\mu\epsilon$) | 3/4" Percent Error | 1" Depth ($\mu\epsilon$) | 1" Percent Error |
|------|-------------------------------|------------------------------|--------------------|----------------------------|------------------|
| 1 | 330 | 301 | 8.8% | 314 | 4.8% |
| 2 | 331 | 298 | 10.0% | 328 | 0.9% |
| 3 | 329 | 325 | 1.2% | 361 | -9.7% |
| 4 | 331 | 297 | 10.3% | 332 | -0.3% |
| | | Average | 7.6% | | -1.1% |

As shown in Table 9, the measured strains were all consistent with the theoretical strains. The relieved strain was used to find the average prestress force at each core location, and then an average was taken for each method used on the beam. The average prestress force calculated from the surface-strain relief method was then compared to the average prestress force determined from the measurement of losses and of the decompression load. Table 10 shows results of the coring method on all six beams. At a core depth of 0.75 inch, larger errors are present and vary from 6% to 24%. A depth of core of one inch shows much less error, with all the beams having an error of less than 10% when compared to the experimentally determined f_{se} .

Table 10 Calculated f_{se} and Percent Error

| Beam | 3/4" Core Depth Calculated f_{se} (ksi) | Percent Error | 1" Core Depth Calculated f_{se} (ksi) | Percent Error | Experimentally Determined f_{se} (ksi) |
|----------|--|------------------|--|------------------|---|
| 1a | 125.1 | 7.2% | 136.4 | -1.2% | 134.8 |
| 1b | 103.2 | 23.6% | 128.9 | 4.5% | 135.0 |
| 2a | 101 | 11.4% | 116.4 | -2.1% | 114.0 |
| 2b | 83.1 | 15.2% | 90.4 | 7.8% | 98.0 |
| T-beam 1 | 110.6 | 14.5% | 119.2 | 7.8% | 129.3 |
| T-beam 2 | 122.7 | 16.0% | 133.5 | 8.6% | 146.0 |

Beams 1a and 1b were cast together in the same prestressing bed, along with beams 2a and 2b. Theoretically, beams 1a and 1b, and 2a and 2b should have the same average prestressing force, so by testing one beam within the first three months after casting, and then testing the second beam at a minimum of six months after casting, the effects of creep and shrinkage on the relieved strain could be examined. When looking at the percent error in Table 10, beams 1b and 2b show larger errors than beams 1a and 2a. This error suggests that creep and shrinkage of the concrete may not be fully relieved through this method. The T-beams tested were approximately nine years old but each shows the surface-strain relief method can accurately determine f_{se} on members older than one year.

The notching procedure was tested on beams 1b, 2a, 2b, and T-beam 2. This procedure showed much larger errors and more variations between beams than with the coring procedure. Table 11 shows results of the notching procedure on the beams tested. Three depths were tested—0.75, one, and 1.25 inches. The finite-element models showed a depth of 1.125 inches provides a full stress relief, but as the data shows in Table 11, a depth of one inch measures a larger relief strain as in beams 2a and 2b, or measures a smaller relief strain

as in beams 1b and T-beam 2. With beams 1b and T-beam 2, an increase in depth to 1.25 inches still did not provide the full stress relief.

Table 11 Calculated f_{se} and Percent Error

| Beam | 3/4" Notch Depth Calculated fse (ksi) | Percent Error | 1" Notch Depth Calculated fse (ksi) | Percent Error | 1.25" Notch Depth Calculated fse (ksi) | Percent Error | Actual |
|----------|--|------------------|--|------------------|---|------------------|--------|
| 1b | 73.1 | 45.9% | 107.6 | 20.3% | 120.6 | 10.7% | 135.0 |
| 2a | 87.9 | 22.9% | 121.0 | -6.1% | 130 | -14.0% | 114.0 |
| 2b | 66.4 | 32.2% | 88.0 | 10.2% | 109.7 | -11.9% | 98.0 |
| T-beam 2 | 97.8 | 33.0% | 124.6 | 14.7% | 132.1 | 9.5% | 146.0 |

CONCLUSIONS

- The core data shows a greater accuracy and precision when compared to the experimentally determined strand stress. The coring process reduces stress influences from the surrounding concrete and creates an almost full stress relief with a core depth of one inch. At a depth of one inch, the core always measured a relief strain less than the actual strain, except on the two members tested before a majority of the losses occurred, which showed an average error of 1.7% larger than the actual strain. The data also agrees with the finite-element models created, which show a depth of one inch balancing the tensile and compressive surface strains out.
- When cutting the core, heat is generated from the friction of the diamond coring bit, which caused an increase in temperature. Due to the size of the beam, the temperature in and around the core reaches equilibrium in about 10 minutes. The strain drift due to temperature is minimal and it takes a few minutes for the gage to stabilize due to the release of strain. Waiting 10 minutes to take the final reading corrects for the temperature error and allows the gage to stabilize.
- The notches provided much more varied results due to the many variables of the method, including notch length, spacing, and depth. For this research, the only variable tested was depth of the notch. From the finite-element models, changing the length or the spacing of the notch changed the measured strain significantly. The finite-element models also showed at a given spacing, a 0.125 inch increase in depth increased the released strain by 24%, whereas an increase in core depth of 0.25 inches resulted in an 18% increase in released strain. When using the coring method, a slight error in depth of the core will not significantly affect the measured strain and will not introduce a large error, as with the notching method. Using the notching method, the errors were larger than that of the cores and also much more varied, ranging from -9% to 22%.
- With each method, some error exists at each location, and it was found that when multiple locations were tested and the average taken, the highest level of accuracy was obtained. Cores or notches need to be taken from both sides to get an average of

the prestressing force in the beam. The notching method provides the benefit of a quicker and simpler method when used with the LSI device. The LSI device eliminates the need to mount strain gages, which is a time-consuming and tedious task. Larger errors exist with the notching procedure, whereas the coring procedure provides a more accurate but a more time-consuming method to determine the average prestress force in a member.

ACKNOWLEDGEMENTS

This work was funded by the Mid-American Transportation Center (MATC) in Lincoln, NE.

REFERENCES

1. ASTM International, "Standard Test Method for Static Modulus of Elasticity and Poisson's Ratio of Concrete in Compression," ASTM C 469, 2002
2. Larson, K., Peterman, R., and Rasheed, H., "Strength-Fatigue Behavior of Fiber Reinforced Polymer Strengthened Prestressed Concrete T-Beams," *Journal of Composites for Construction*, V. 9, No. 4, July-August 2005, pp. 313-326
3. Kaczinski, M., Pessiki, S., and Wescott, H., "Evaluation of Effective Prestress Force in 28-Year-Old Prestressed Concrete Bridge Beams," *PCI Journal*, November-December 1996, pp. 78-89
4. Larson, K., "Behavior of FRP Strengthened Reinforced Prestressed Concrete Girders in Flexure, Shear, and Delimitation," MS Thesis, Civil Engineering, Kansas State University, Manhattan, 2002
5. Halsey, T., and Miller, R., "Destructive Testing of Two Forty-Year-Old Prestressed Concrete Bridge Beams," *PCI Journal*, September-October 1996, pp. 84-93
6. Zhao, W., "Development of a Portable Optical Strain Sensor with Applications in Diagnostic Testing of Prestressed Concrete," Ph.D. Dissertation, Mechanical and Nuclear Engineering, Kansas State University, Manhattan, 2011
7. Vishay Micro-Measurements, "Strain Gage Selection: Criteria, Procedures, Recommendations," *Strain Gage Technology Technical Data*, August 2007
8. McGinnis, M., "Experimental and Numerical Development of the Core-Drilling Method for the Nondestructive Evaluation of In-situ Stresses in Concrete Structures," Ph.D. Dissertation, Civil and Environmental Engineering, Lehigh University, Bethlehem, 2006
9. Marks, D., "Development of Residual Stress Measurement for Concrete Pavements Through Cantilevered Beam Testing," MS Thesis, Civil Engineering, University of Illinois at Urbana-Champaign, 2009
10. Vishay Micro-Measurements, "Strain Gage Thermal Output and Gage Factor Variation with Temperature," *Strain Gage Technology Technical Data*, August 2007